https://doi.org/10.2352/EI.2022.34.10.IPAS-193

Optimal parameters selection of the Frost filter based on despeckling efficiency prediction for Sentinel SAR images

Oleksii Rubel, National Aerospace University, 61070, Kharkiv, Ukraine
Andrii Rubel, National Aerospace University, 61070, Kharkiv, Ukraine
Vladimir Lukin, National Aerospace University, 61070, Kharkiv, Ukraine
Karen Egiazarian, Tampere University, FIN 33101, Tampere, Finland

Abstract

Synthetic aperture radar (SAR) images have found numerous applications. However, analysis of SAR images including interpretation, classification, segmentation, etc. is an extremely challenging task due to the presence of intensive speckle noise. Therefore, image denoising is one of the main stages in SAR data pre-processing. Over the past decades, a large number of different image denoising techniques have been proposed ranging from local statistics filters to deep learning based ones. In this study, we analyze one of the most known and widely used local statistics Frost filter. Despeckling efficiency of the Frost filter significantly depends on the sliding window size and tuning (also called damping) factor. Here, we present a method for optimal parameters selection of the Frost filter for a given image based on despeckling efficiency prediction. Despeckling efficiency prediction is carried out using a set of statistical and spectral input parameters and a multilayer neural network. It is shown that such a prediction can be performed before applying image despeckling with a high accuracy and it is faster than despeckling itself. Both simulated speckled images and real-life Sentinel-1 SAR images have been used for extensive evaluation of the proposed method.

Introduction

It is well known that radar images are widely used in various remote sensing applications [1, 2]. The main advantage of radar imaging is its ability to operate and collect data regardless of cloudiness, weather and lighting conditions [2]. However, radar images are corrupted by a noise-like phenomenon called speckle [2, 3]. It is caused by the coherent interference of reflected signals from a large number of elementary reflectors within a resolution cell [1]. The presence of intensive speckle noise especially in modern synthetic aperture radars (SARs) affects the efficiency of different high-level processing steps like classification or segmentation. Thus, it is desirable to suppress speckle in order to improve SAR image interpretability.

A huge number of various filters has been developed to suppress speckle noise [3-7]. At the same time, it is still challenging to choose which filter is better to apply and how to select its parameters. Many factors influence a filter speckle suppression efficiency. One possible way to increase despeckling efficiency is to select optimal parameters for a given filter taking into account image properties and speckle characteristics. Several methods have been proposed for selection of filter parameters [8-10]. In [8], adaptive windowing approach has been proposed where the window size is automatically adjusted according to image characteristics (homogeneous or heterogeneous regions) for local statistics Mean and Lee filters. In [9], a method of adaptive adjusting of the tuning factor and the size of sliding window for the local statistics Frost filter has been proposed depending on the regional characteristics to get a balance between speckle suppression and edge preservation.

In this paper we consider the Frost filter [7] since it is still widely used in various toolboxes like SNAP [11]. Our previous studies have shown that it is possible to predict despeckling efficiency beforehand with high accuracy for several filters [12]. We have already demonstrated how to select the window size for the well-known local statistics Lee filter based on despeckling efficiency prediction [10]. Therefore, we demonstrate here that such an approach can be extended to the Frost filter that has two adjustable parameters, with application to real-life Sentinel-1 SAR images in order to provide a better trade-off between speckle suppression and edge/detail preservation.

Adaptive Parameters Selection for the Frost Filter

Before starting the description of the proposed approach, let us briefly recall radar image model. Speckle noise is known to be pure multiplicative [1, 3]. The observed radar image model is described as:

$$I^{n}(i,j) = I^{true}(i,j) \cdot \mu(i,j)\,, \tag{1}$$

where $I^{n}(i,j)$ is the ij-th speckled image pixel, $I^{true}(i,j)$ denotes noise-free image pixel, $\mu(i,j)$ is a random variable with Gamma distribution (or Rayleigh distribution for single look amplitude images) with mean equal to unity and relative variance σ_{μ}^{2} modeling the speckle. In [13], it has been shown that relative variance of speckle σ_{μ}^{2} for Interferometric Wide (IW) swath mode GRD Sentinel-1 SAR images is approximately equal to 0.05 for both polarization modes VV and VH.

Recall that output for the Frost filter is described as follows [7, 9]:

$$I^{Frost}(i,j) = \sum_{s}\sum_{h} P_{sh} m_{sh} \Big/ \sum_{s}\sum_{h} m_{sh}\,,\quad m_{sh} = e^{-KC_I^2 d_{sh}} \tag{2}$$

where $I^{Frost}(i,j)$ is the ij-th despeckled image pixel, P_{sh} is the pixel values in the local window centered at the ij-th pixel (s and h are indices of pixels within the local window), K ($K > 0$) denotes tuning factor (or the so-called damping factor), C_I denotes coefficient of variation defined as the ratio of the sample standard deviation to the sample mean of the pixels in the local window, d_{sh} is the distance from the centered pixel to the neighboring pixels in the local window. The value of tuning factor K influences the trade-off between speckle suppression and edge preservation.

It is also worth noting that in this study the peak signal-to-noise ratio (PSNR), PSNR-HVS-M [14] and FSIM [15] image quality measures are used to assess despeckling efficiency for the Frost filter. More in detail, despeckling efficiency is described by a value of improvement due to despeckling for a given image quality measure, i.e. a difference for a given image quality measure after and before applying despeckling [10, 12]. Both PSNR and PSNR-HVS-M image quality measures are expressed in dB, where larger values correspond to better image quality. Values for FSIM measure vary from 0 to 1, larger values relate to better image quality.

Despeckling Efficiency Prediction for the Frost Filter

In this subsection, we describe an approach to predict despeckling efficiency for the Frost filter with different settings, i.e. window size and damping factor, using a set of input parameters extracted from a given speckled image and a multilayer neural network as a regressor. In this study, we have considered five window sizes: 5x5, 7x7, 9x9, 11x11, 13x13 pixels and the damping factor (DF) varied from 1 to 3 with the step 0.5.

Extracted Input Parameters

Here we utilized the same approach and set of statistical and spectral input parameters as in our previous research [10]. Now we briefly describe four groups of input parameters.

The first group is energy allocation parameters calculated in the discrete cosine transform (DCT) domain. A normalized spectral power is determined in four spectral sub-bands of 8x8 pixel blocks (see Fig. 1) denoted by digits from 1 to 4 as follows [12]:

$$W_m = \frac{\sum_{k,l \in S_m} D_{kl}^2}{\sum_{k=1}^{8} \sum_{l=1}^{8} D_{kl}^2 - D_{11}^2} \qquad (3)$$

where D_{kl} denotes a DCT coefficient with indices k and l in a block ($k = 1..8,\ l = 1..8$), m is an index of the m-th sub-band S_m ($m = 1..4$), W is a normalized energy allocation parameter that lies in the range from 0 to 1.

0	1	1	1	1	2	2	2
1	1	1	1	2	2	2	3
1	1	1	2	2	2	3	3
1	1	2	2	2	3	3	3
1	2	2	2	3	3	3	4
2	2	2	3	3	3	4	4
2	2	3	3	3	4	4	4
2	3	3	3	4	4	4	4

***Figure 1**. Four spectral sub-bands in the 2D DCT domain*

Then, for the obtained set of W_m for each sub-band, four statistical parameters, namely mean, variance, skewness and kurtosis have been calculated. Totally 16 parameters representing energy allocation in the DCT blocks have been obtained.

The second group of input parameters includes four blocks' parameters. They describe image statistics in 8x8 pixel blocks. These four parameters are mean, variance, skewness, and kurtosis of block means distribution [10].

Another group is the so-called probability parameters. For each 8x8 DCT block, the probabilities $P_\sigma(q)$, $q = 1,..,Q$ in a q-th block (Q is a total number of analyzed blocks), where magnitudes of DCT coefficients are smaller than the corresponding thresholds [12]:

$$T_{q\,kl} = \sigma_\mu \bar{I}_q \sqrt{D_{pn}(k,l)}, \qquad (4)$$

where $D_{pn}(k,l)$ denotes the DCT normalized power spectrum, $\bar{I}_q$ is the q-th block mean, σ_μ^2 is the relative variance of the speckle. Note that in our study σ_μ^2 is equal to 0.05. Next, after getting all estimates $P_\sigma(q),\ q = 1,..,Q$, four statistical parameters, i.e. mean, variance, skewness, and kurtosis have been calculated.

The last group of input parameters consists of four global statistics parameters. These parameters are calculated as mean, variance, skewness and kurtosis for the whole analyzed image.

Finally, all above-mentioned 28 parameters can be potentially used to train neural network, although our experiments have shown that it is enough to use 13 parameters without losing prediction performance [10].

Neural Network Structure and its Training

Prediction of despeckling efficiency in terms of improvement for a given image quality measure for the Frost filter is carried out using the multilayer perceptron (MLP) and 13 input parameters extracted from an analyzed speckled image. It consists of three hidden layers with hyperbolic tangent activation function. Bayesian regularization backpropagation has been used to train multilayer perceptron and 30 epochs have been established. The output of the used MLP is a value of improvement for a given image quality measure. The architecture of the used neural network is shown in Fig.2.

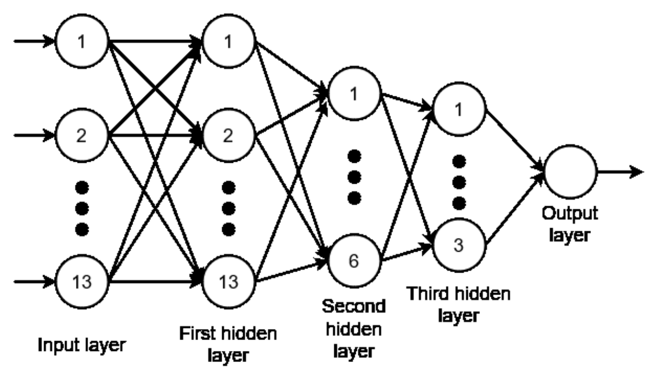

***Figure 2**. Architecture of the multilayer perceptron used to perform prediction of despeckling efficiency (improvement for a given image quality measure) for the Frost filter*

We have used 100 high quality component images from #5 and #11 channels of multispectral data acquired by Sentinel-2 to create a dataset for neural network training and validation. Each component image from both channels was divided into images of the size 512x512 pixels. As a result, 8100 images of 512x512 pixels for each channel were used as speckle-free (reference) images. These images were then distorted by artificially generated speckle with the same properties as for Sentinel-1 SAR images and filtered by the Frost filter with different window sizes and damping factors.

The data for neural network training and validation were collected in the following way. First, for all images distorted by the speckle, the statistical and spectral input parameters were calculated and saved. In addition, using speckled images and the corresponding reference ones, the values of the considered image quality measures, namely PSNR, PSNR-HVS-M, and FSIM were obtained. For despeckled images, the corresponding measure values were obtained in the same way. The values of improvement due to despeckling (difference between measure values for despeckled images and for the corresponding noisy ones) for all image quality measures were determined as well. Here and below we denote the improvement for the considered image quality measures as IPSNR, IPHVSM and IFSIM.

The procedure of neural network training and validation has been conducted in two stages. At the first stage, which is called self-dataset validation, the dataset was divided into two parts: 80% of images have been used for training and the remaining 20% of images for validation. In this stage, all images have been taken from one channel, namely #5. The second stage using cross-validation has been performed to evaluate the generalization capability of the trained neural network. To perform cross-validation, the image dataset has been divided in the same proportion, but the training subset of 80% of images (i.e. 6480 images) has been taken from channel #5, while other part of 20% of images (i.e. 1620 images) from channel #11 has been utilized for validation. The procedure of random splitting the dataset into training and validation subsets has been carried out 100 times.

Prediction Accuracy

To evaluate the prediction accuracy of despeckling efficiency for the Frost filter, the adjusted coefficient of determination $\bar{R}^2$ [16] averaged over 100 realizations of train-validation splitting procedure was used. Note that the values of adjusted $\bar{R}^2$ vary from 0 to 1, where the higher the value of $\bar{R}^2$, the more accurate the prediction is.

The self-dataset along with cross-dataset validation results for IPSNR, IPHSVM and IFSIM image quality measures are given in Tables 1-3.

Table 1: Prediction accuracy for IPSNR

Self-dataset evaluation					
Adjusted $\bar{R}^2$					
DF / Window size	**5x5**	**7x7**	**9x9**	**11x11**	**13x13**
1	0.976	0.975	0.974	0.973	0.971
1.5	0.981	0.979	0.978	0.976	0.974
2	0.983	0.982	0.980	0.978	0.976
2.5	0.984	0.983	0.982	0.980	0.977
3	0.985	0.984	0.982	0.980	0.978
Cross-dataset evaluation					
Adjusted $\bar{R}^2$					
DF / Window size	**5x5**	**7x7**	**9x9**	**11x11**	**13x13**
1	0.949	0.954	0.959	0.963	0.967
1.5	0.956	0.961	0.965	0.969	0.971
2	0.960	0.966	0.970	0.973	0.975
2.5	0.964	0.970	0.975	0.977	0.979
3	0.965	0.972	0.977	0.980	0.981

One can see that the prediction is very accurate. In case of self-dataset evaluation for all considered measures, the values of adjusted $\bar{R}^2$ are in the range from 0.945 to 0.985. Analysis of the obtained results for the cross-dataset evaluation also shows that the values of adjusted $\bar{R}^2$ have decreased by 0.02-0.05 compared to the corresponding results for self-dataset evaluation. It is especially noticeable in the case of improvement prediction for IPHVSM measure. In general, the prediction accuracy is still very high. Thus, we can conclude that the trained neural network demonstrates high generalization capability and stable results.

Table 2: Prediction accuracy for IPHVSM

Self-dataset evaluation					
Adjusted $\bar{R}^2$					
DF / Window size	**5x5**	**7x7**	**9x9**	**11x11**	**13x13**
1	0.957	0.956	0.955	0.954	0.953
1.5	0.964	0.962	0.960	0.958	0.956
2	0.962	0.959	0.956	0.953	0.951
2.5	0.960	0.956	0.953	0.950	0.947
3	0.958	0.953	0.950	0.947	0.945
Cross-dataset evaluation					
Adjusted $\bar{R}^2$					
DF / Window size	**5x5**	**7x7**	**9x9**	**11x11**	**13x13**
1	0.894	0.901	0.908	0.913	0.918
1.5	0.948	0.956	0.961	0.964	0.964
2	0.958	0.964	0.966	0.966	0.963
2.5	0.958	0.962	0.962	0.959	0.955
3	0.957	0.958	0.955	0.951	0.946

Table 3: Prediction accuracy for IFSIM

Self-dataset evaluation					
Adjusted $\bar{R}^2$					
DF / Window size	**5x5**	**7x7**	**9x9**	**11x11**	**13x13**
1	0.982	0.982	0.983	0.982	0.982
1.5	0.981	0.982	0.982	0.982	0.982
2	0.976	0.977	0.978	0.978	0.978
2.5	0.973	0.973	0.973	0.972	0.972
3	0.969	0.968	0.966	0.965	0.964
Cross-dataset evaluation					
Adjusted $\bar{R}^2$					
DF / Window size	**5x5**	**7x7**	**9x9**	**11x11**	**13x13**
1	0.941	0.943	0.944	0.944	0.944
1.5	0.961	0.963	0.965	0.965	0.966
2	0.959	0.960	0.960	0.960	0.960
2.5	0.950	0.948	0.946	0.944	0.944
3	0.940	0.933	0.928	0.925	0.925

Filter Parameters Selection

As has been shown above, the despeckling efficiency for the Frost filter can be accurately predicted for a set of filter parameters' values, i.e. the window size and damping factor. Based on this prediction, it is possible to choose what values of the filter parameters to set for a considered speckled image.

Our approach to filter parameters selection is based on predicting the values of improvement for a given image quality measure, e.g. IPSNR, IPHVSM or IFSIM, for different scanning window sizes and damping factor values, and selecting the corresponding parameters for which the predicted image quality measure improvement is the largest. It is possible because such a prediction is much faster than despeckling itself.

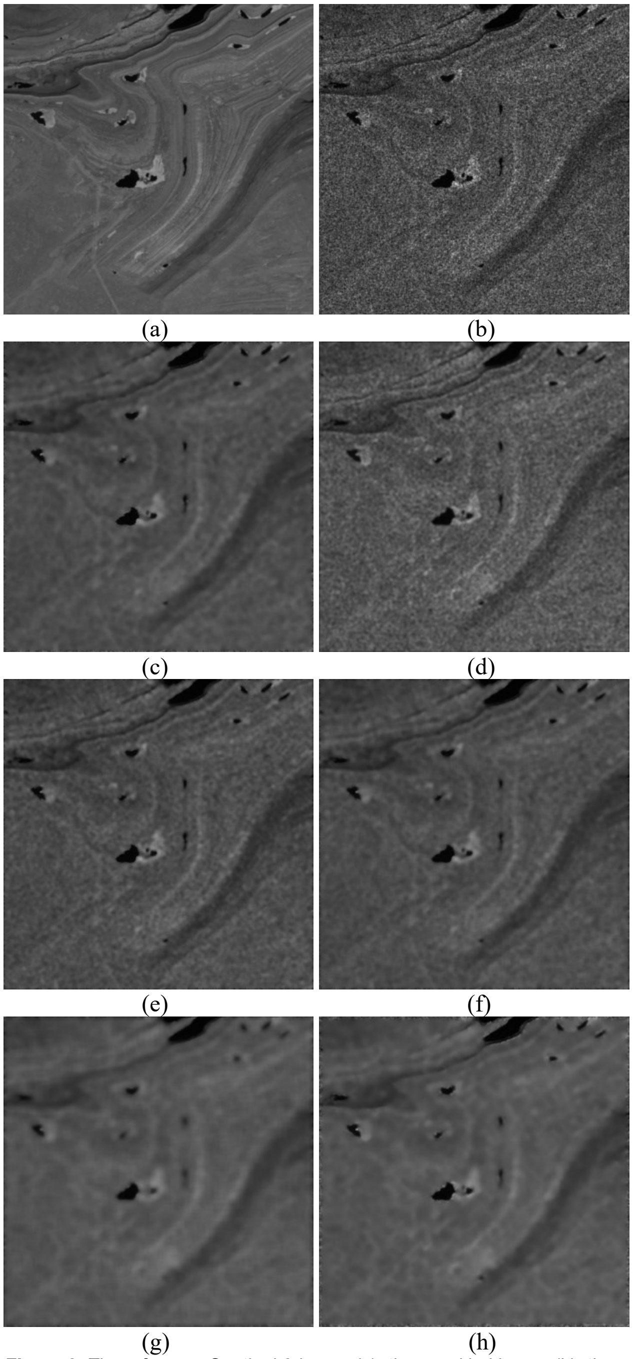

***Figure 3**. The reference Sentinel-2 image (a); the speckled image (b); the optimal filter output for the 11x11 window size and DF = 3 (c); the filter output for the 5x5 window size and DF = 1 (d); the filter output for the 7x7 window size and DF = 2.5 (e); the filter output for the 9x9 window and DF = 2 (f); the filter output for the 13x13 window and DF = 1 (g); the filter output for the 13x13 window and DF = 3 (h)*

Let us show an example of the test image artificially distorted by the speckle and the selected filter parameters depending on the predicted improvements of image quality measures. Fig. 3 shows the reference Sentinel-2 image (a), the speckled image (b), and the Frost filter outputs for different parameters (c-h).

The ground-truth values of improvement for all considered measures for the above test image with different filter parameters (not all shown) are given in Table 4. The values of PSNR, PSNR-HVS-M and FSIM measures for the image artificially distorted by speckle (see Fig. 3 b) are 22.043 dB, 19.2707 dB and 0.7013, respectively. It can be observed from the data in Table 4 that the 11x11 window size and DF=3 are the best parameters. It is consistent with visual inspection. The predicted values for the 11x11 window size and DF = 3 are IPSNR = 8.64 dB, IPHVSM = 6.91 dB and IFSIM = 0.1753. All predicted values are very close to the corresponding ground-truth (see Table 4), which confirms that our trained neural network predicts quite accurately.

Table 4: Ground-truth values of improvement for IPSNR, IPHVSM and IFSIM image quality measures

Filter Parameters	IPSNR, dB	IPHVSM, dB	IFSIM
5x5, DF = 1	6.5389	4.2869	0.12813
7x7, DF = 2.5	7.9012	5.8478	0.1679
9x9, DF = 2	8.2362	6.2635	0.17152
11x11, DF = 3	**8.6065**	**6.7721**	**0.17234**
13x13, DF = 1	7.2657	5.126	0.10983
13x13, DF = 3	8.5305	6.7167	0.14623

Now let us give a real-life example. Fig. 4 shows an example for real Sentinel-1 SAR image of size 512x512 pixels and the Frost filter output with the selected window size 13x13 and DF = 1. The values of the predicted measures IPSNR, IPHVSM and IFSIM for different filter parameters are given in Table 5. According to the obtained result, the window size of 13x13 and DF=1 provide the best results for all image quality measures. The best values are highlighted.

Let us also compare despeckling efficiency of the Frost filter with the Lee filter [10] for which the optimal parameters are chosen in accordance with IPHVSM image quality measure. Values of improvement for IPHVSM measure for different parameters and for both Frost and Lee filters are given in Table 6. The test Sentinel-2 image along with the outputs for both filters with optimal parameters are shown in Fig. 5.

Table 6: Values of improvement for IPHVSM for different parameters for the Frost and Lee filters

Frost filter					
IPHVSM, dB					
DF / Window size	**5x5**	**7x7**	**9x9**	**11x11**	**13x13**
1	4.0307	4.1126	4.1813	4.2270	4.2463
1.5	4.7309	4.9817	5.1775	5.3016	5.3608
2	4.7020	5.1151	5.4156	5.6002	**5.6983**
2.5	4.4857	5.0001	5.3515	5.5656	5.6912
3	4.2603	4.8236	5.1912	5.4188	5.5644
Lee filter					
IPHVSM, dB					
Window size	**5x5**	**7x7**	**9x9**	**11x11**	**13x13**
	4.4516	**5.2458**	**5.0570**	4.6081	4.1649

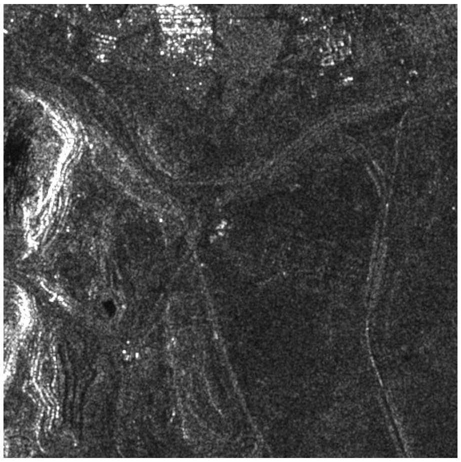

(a)

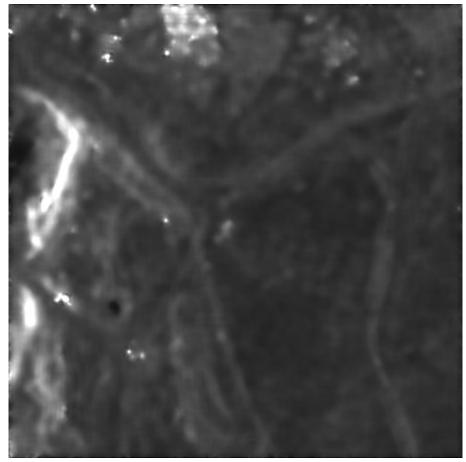

(b)

Figure 4*. The original Sentinel-1 SAR image (a) and the Frost filter output with the selected window size 13x13 and DF=1 (b)*

Table 5: Predicted results of the Frost filter for real-life Sentinel-1 SAR image

Predicted IPSNR, dB					
DF / Window size	**5x5**	**7x7**	**9x9**	**11x11**	**13x13**
1	2.0383	2.256	2.4614	2.6465	**2.8084**
1.5	1.0833	1.4753	1.8379	2.1609	2.4428
2	0.3586	0.8989	1.3883	1.8175	2.1866
2.5	-0.149	0.5189	1.1107	1.6196	2.0481
3	-0.5049	0.2738	0.9489	1.5164	1.9828
Predicted IPHVSM, dB					
1	1.4996	1.6953	1.8725	2.0298	**2.1646**
1.5	0.2466	0.64169	1.008	1.3303	1.6055
2	-0.74942	-0.19896	0.21594	0.70322	1.1543
2.5	-1.4403	-0.87831	-0.013033	0.32467	0.81137
3	-1.6964	-1.1584	-0.57176	0.35976	0.69621
Predicted IFSIM					
1	0.028442	0.030256	0.031687	0.032965	**0.034271**
1.5	0.0035402	0.0085051	0.012819	0.016662	0.020158
2	-0.027686	-0.019203	-0.01166	-0.0047607	0.0013743
2.5	-0.05424	-0.042614	-0.031899	-0.022133	-0.013334
3	-0.075988	-0.061304	-0.047535	-0.034978	-0.023768

Analysis of the results in Table 6 shows that optimal window size and damping factor for the Frost filter are 13x13 and 2, respectively, while for the Lee filter the 7x7 window size is the best. It is well seen that the Frost filter with optimal parameters outperforms the Lee filter both in visual quality and in improvement of IPHVSM measure.

Conclusions

In this paper, a method for selection of parameters of the well-known Frost filter is presented. The novelty of the proposed method and obtained results consists in the following: 1) it is possible to perform despeckling efficiency prediction for the Frost filter using statistical and spectral parameters extracted from an analyzed speckled image and employed neural network before applying despeckling itself very quickly and quite accurately (coefficient of determination is larger than 0.9); 2) it is demonstrated that such a prediction can be done for several image quality measures utilized to characterize the image despeckling efficiency; 3) it is shown how to properly select the sliding window size and damping factor for the Frost filter according to different image quality measures based on despeckling efficiency prediction; 4) the proposed method of selection parameters for the Frost filter is adopted to speckle characteristics for real-life Sentinel-1 SAR images.

References

[1] C. Oliver and S. Quegan, “Understanding Synthetic Aperture Radar Images”, SciTech Publishing. 2004, 486 p.

[2] J.-S. Lee, E. Pottier, “Polarimetric Radar Imaging: From Basics to Applications,” CRC Press, 2009, 422 p.

[3] R. Touzi, “A review of speckle filtering in the context of estimation theory,” in IEEE Transactions on Geoscience and Remote Sensing, vol. 40, no. 11, pp. 2392-2404, Nov. 2002, doi: 10.1109/TGRS.2002.803727.

[4] J. Lee, T. L. Ainsworth and Y. Wang, “A review of polarimetric SAR speckle filtering,” in Proc. 2017 IEEE International Geoscience and Remote Sensing Symposium (IGARSS), Fort Worth, TX, 2017, pp. 5303-5306, doi: 10.1109/IGARSS.2017.8128201.

[5] C.A. Deledalle, L. Denis, S. Tabti, F. Tupin, “MuLoG, or how to apply Gaussian denoisers to multi-channel SAR speckle reduction?,” in IEEE Transactions on Image Processing, vol. 26, no. 9, pp. 4389-4403, 2017.

[6] J. -S. Lee, “Digital Image Enhancement and Noise Filtering by Use of Local Statistics,” in IEEE Transactions on Pattern Analysis and Machine Intelligence, vol. PAMI-2, no. 2, pp. 165-168, March 1980, doi: 10.1109/TPAMI.1980.4766994.

[7] V. S. Frost, J. A. Stiles, K. S. Shanmugan and J. C. Holtzman, “A Model for Radar Images and Its Application to Adaptive Digital Filtering of Multiplicative Noise,” in IEEE Transactions on Pattern Analysis and Machine Intelligence, vol. PAMI-4, no. 2, pp. 157-166, March 1982, doi: 10.1109/TPAMI.1982.4767223.

[8] J. M. Park, W. J. Song and W. A. Pearlman, “Speckle filtering of SAR images based on adaptive windowing,” IEE Proc.-Vis. Image Signal Process., vol. 146, no. 4, pp. 191-197, Aug. 1999.

[9] Z. Sun, Z. Zhang, Y. Chen, S. Liu and Y. Song, “Frost Filtering Algorithm of SAR Images with Adaptive Windowing and Adaptive Tuning Factor,” in IEEE Geoscience and Remote Sensing Letters, vol. 17, no. 6, pp. 1097-1101, June 2020, doi: 10.1109/LGRS.2019.2939208.

[10] O. Rubel, V. Lukin, A. Rubel, and K. Egiazarian, “Selection of Lee Filter Window Size Based on Despeckling Efficiency Prediction for Sentinel SAR Images,” Remote Sensing, vol. 13, no. 10, p. 1887, May 2021.

[11] “Science Toolbox Exploitation Platform (STEP),” SNAP Toolbox. [Online]. Available: https://step.esa.int/main/download/snap-download/. [Accessed: 22-Nov-2021].

[12] O. Rubel, V. Lukin, A. Rubel, and K. Egiazarian, “NN-Based Prediction of Sentinel-1 SAR Image Filtering Efficiency,” Geosciences, vol. 9, no. 7, p. 290, Jun. 2019, doi: 10.3390/geosciences9070290.

[13] V. Abramova, S. Abramov, V. Lukin and K. Egiazarian, “Blind estimation of speckle characteristics for Sentinel polarimetric radar images,” 2017 IEEE Microwaves, Radar and Remote Sensing Symposium (MRRS), 2017, pp. 263-266, doi: 10.1109/MRRS.2017.8075078.

[14] N. Ponomarenko, F. Silvestri, K. Egiazarian, M. Carli, J. Astola, and V. Lukin, “On between-coefficient contrast masking of DCT basis functions,” in Proc. 3rd Int. Workshop Video Process. Qual. Metrics Consum. Electron, Scottsdale, USA, Jan. 2007, 4 p.

[15] L. Zhang, L. Zhang, X. Mou and D. Zhang, “FSIM: A Feature Similarity Index for Image Quality Assessment,” in IEEE Transactions on Image Processing, vol. 20, no. 8, pp. 2378-2386, Aug. 2011, doi: 10.1109/TIP.2011.2109730.

[16] A.C. Cameron and F. Windmeijer, “An R-squared measure of goodness of fit for some common nonlinear regression models,” Journal of Econometrics, vol. 77, no. 2, pp. 329-342, April 1997.

Author Biography

Andrii Rubel received his M.S. in telecommunications from the Kharkiv National University of Radioelectronics, in 2016. He received his Ph.D. in Remote Sensing from the National Aerospace University named after M.E. Zhukovsky, in 2021.

Oleksii Rubel received his M.S. in telecommunications from the National Aerospace University named after M.E. Zhukovsky, in 2013. He received his Ph.D. in Remote Sensing from the National Aerospace University named after M.E. Zhukovsky, in 2016.

Vladimir Lukin received his Ph.D. in 1988 and Doctor of Technical Science in remote sensing from the National Aerospace University named after M.E. Zhukovsky, Ukraine, in 2002. Since 1995, he has been in cooperation with Tampere University of Technology. Currently he is a head of the Department of Information and Communication Technologies and a professor.

Karen Egiazarian received his Ph.D. from Moscow M. V. Lomonosov State University, Russia, in 1986, and his Doctor of Technology in signal processing from Tampere University of Technology, Finland, in 1994. He is leading a “Computational imaging” group and a professor at the Department of Computing Sciences, Tampere University, Tampere, Finland. He is an IEEE Fellow, and a member of the DSP Technical Committee of the IEEE Circuits and Systems Society.

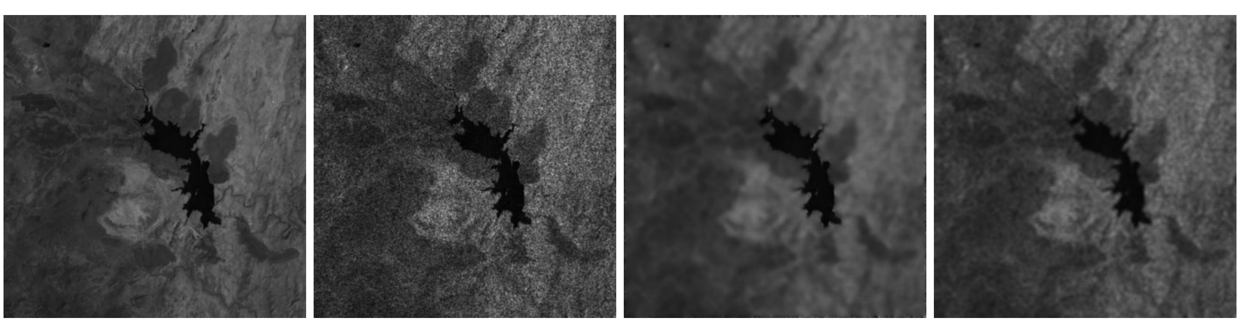

(a) (b) (c) (d)

Figure 5. The reference Sentinel-2 image (a); the speckled image (b); the Frost filter output with the 13x13 window size and DF=2 (c); the Lee filter output with the 7x7 window size (d)